

CHARGE-COUPLED DEVICE INTEGRATION-TIME CODING FOR DETECTION  
OF IMAGES MOVING WITH UNKNOWN VELOCITIES

J. M. White  
G. W. Lynch

IBM Thomas J. Watson Research Center  
Yorktown Heights, New York 10598

ABSTRACT

Existing techniques for the detection of a moving low light level image by a CCD array have required velocity synchronism between the image and the photogenerated charges. This was necessary to prevent blurring during the long duration of charge integration. A new detection scheme is described which causes the image to be convolved with a clock modulation signal as the photocharges are collected. The charge accumulating from each image point will now be spread over many photoelements due to the absence of velocity synchronism, but the output is not blurred in the usual sense. Instead the charge is distributed through the array in a controlled way so that the image can be reconstructed.

I. INTRODUCTION

The applications of charge coupled devices (CCD's) and other charge transfer devices have burgeoned into areas such as image sensing, electronic signal processing, and digital memories [Ref. 1]. One particular area of interest unique to charge transfer devices is image processing in which functions of sensing and processing may be effectively combined. One example of this combination is time delay and integration (TDI) [Ref. 2,3] in which the detection of an optical image moving at known velocity is improved by being averaged over many photocells as a result of synchronization of the motion of the charges in the CCD with the motion of the image for the duration of a long integration period. Also, Lagnado and Whitehouse [Ref. 4] have described ways of combining multiplication with the functions of time delay and optical integration so that image convolution can be achieved with CCD circuitry. Extending these ideas, we describe the use of a CCD linear scanner array to obtain the convolution of a moving optical image with discretely sampled linear FM chirps. This allows reconstruction of the image even though it was originally scanned while moving at an unknown velocity.

II. CONCEPTS OF OPERATION

Two primary ideas have been combined in our detection technique. The first concept gives a means for recording the convolution of the optical image with an electronic reference signal. An important part of this first concept is that the image is always moving relative to the accumulated charge packets. Synchronization of image and charge motion (as in TDI) is not needed and, in fact, must be avoided. The second concept relies on unique properties of the linear FM chirp as a reference signal. These properties have been studied in detail for applications such as RADAR signal processing (Ref. 5). The results of such studies can be used to give an indication of the ultimate capabilities of the chirp convolution detection technique.

A. CONVOLUTION VIA INTEGRATION CLOCK TIMING MODULATION

It is possible to take a slowly varying reference signal  $r(t)$ , sample its amplitude, and use this value to control the integration timing cycle of a CCD photoarray. Furthermore, with two storage cells at each photoelement, it is possible to assign positive and negative values to the weighting function  $r(t)$ . In this case, the integration periods are split, based on the value of  $r(t)$ . After the first part of each cycle the charge in a particular photoelement is put into one cell, and after the remainder of the cycle, the additional charge is put into the other cell. The difference between charge collected in the arrays of cells during one integration cycle then represents the product of the image intensity  $i(x,t)$  and the reference signal. If the photocharge is collected for many cycles without being shifted out of the storage cells, the difference between the linear charge per unit length in the "positive" and "negative" arrays becomes

$$q(x,t) = w \int_{-\infty}^t i(x-v_i t') r(t') dt' \quad (1)$$

Image intensity distribution  $i$  is moving with constant velocity  $v_i$  and is in units of photocurrent collected per unit area.  $w$  is the transverse width of the photoarray. The dimensionless weighting function  $r$  and the array elements are assumed to be suitably approximated by the continuous limit so that the charge may be written as an integral instead of a sum of discrete elements. Equation (1) is recognized as the convolution of the image and reference functions within the spatial and temporal limits of the device.

The convolutional distribution of charge may be collected as described in the above paragraphs, and the integrated values then shifted, or read, out of the array. However, the shifting can also be accomplished simultaneously with the collection of photocharge. This mode of operation is somewhat similar to TDI, but one important difference is that the image velocity  $v_i$  and the velocity of the collected charge  $v_c$  are unequal. The shift of charge along the array during the integration process is equivalent to replacing  $x$  by  $x - v_c(t - t')$  in integrand of Eqn. (1), which gives

$$q(x,t) = w \int_{-\infty}^t i[(x-v_c t) - (v_i - v_c)t'] r(t') dt' \quad (2)$$

The variable of integration can be changed,

$t' \rightarrow \frac{x'}{\Delta v}$  where  $\Delta v = v_i - v_c$ , to give

$$q(x, t) = \frac{w}{\Delta v} \int_{-\infty}^{\Delta v \cdot t} i[(x - v_c t) - x'] r\left[\frac{x'}{\Delta v}\right] dx'. \quad (3)$$

Equation 3 represents the convolution of the image function with a modified version of the reference signal. Moving the charge during the integration process is seen to be equivalent to expanding or shrinking the scale of the reference function.

#### B. THE LINEAR FM CHIRP AS THE REFERENCE SIGNAL

If the reference signal  $r(t)$  is chosen to be a linear FM chirp, then the image  $i(x)$  can be reconstructed from the convolved charge distribution which was recorded in the CCD. The reconstruction is achieved by passing the CCD output through an appropriate matched filter having a compensating linear dispersion. This is straightforwardly demonstrated by an analysis in the frequency (Fourier transform) domain.

The frequencies associated with the linear FM chirp are linearly and uniformly dispersed in time; therefore, a matched filter having a compensating linear dispersion will cause the chirp to be compressed into a narrow spike, or delta function.

In complex analog notation, the linear FM chirp, called  $r$  for "reference" signal, is

$$r(t) = \exp j \left[ (\omega_0 + \frac{\mu t}{2}) t \right] \quad (4)$$

which has an instantaneous frequency described by constants  $\omega_0$  and  $\mu$ . The Fourier transform of this  $r(t)$  is

$$R(\omega) = \sqrt{\frac{\pi}{|\mu|}} \exp -j \left[ \frac{(\omega - \omega_0)^2}{2\mu} \right]. \quad (5)$$

A capitalized function name indicates frequency domain representation of the respective lower-case time domain function name. If the above signal  $R(\omega)$  is passed through a filter having a transfer function

$$H(\omega) = \sqrt{\frac{\pi}{|\mu|}} \exp j \left[ \frac{(\omega - \omega_0)^2}{2\mu} \right] \quad (6)$$

(i.e., identical to  $R(\omega)$  but with opposite sign of dispersion,  $\mu \rightarrow -\mu$ ) then the output will be constant in the frequency domain:

$$R(\omega) \cdot H(\omega) = \frac{\pi}{|\mu|}. \quad (7)$$

Thus, in the time domain, the output will be a spike, or delta function.

The output of the CCD described in section II A is the convolution of the image function and the reference function. In the frequency domain, the convolution becomes a multiplication:

$$Q(\omega) = I(\omega) \cdot R(\omega). \quad (8)$$

When passed through the filter  $H(\omega)$ , the final output  $G(\omega)$  is

$$G(\omega) = I(\omega) \cdot R(\omega) \cdot H(\omega) = I(\omega) \cdot \frac{\pi}{|\mu|}. \quad (9)$$

Thus, the output of the filter equals the input image function except for an amplitude constant. The image function is recovered even though it had been spread out due to the difference in velocities between image and charge motions.

Of course, the above analysis is idealized. In actuality, the length of the CCD and the time scales used are bounded and discrete, and the functions  $i(x)$  and  $r(t)$  are real. The use of a real, finite length, sampled chirp restricts the resolution and quality of the final compressed image which is recovered [Ref. 5] and the frequency range which may be utilized [Ref. 6]. However, the analysis indicates the essential concepts of operation.

### III. EXPERIMENTAL DEVELOPMENT

The demonstration of our convolution techniques in a commercially available product, the CCD110 (Fairchild Semiconductor Components Arrays, Fairchild Camera and Instrument Corporation, Mountainview, California) required construction of circuitry to provide a set of waveforms, Fig. 1, which are different from those used for the CCD110 in normal image scanning operations.

Convolution of the spatial variation of the optical signal with the temporal variation of a discrete sampled analog reference signal requires multiplication of the optical signal by the reference signal. Multiplication is accomplished by converting the amplitude of the sampled analog reference into a clocking sequence where charge integration time is proportional to the reference amplitude. The reference analog signal is sampled with period  $T = 20 \mu s$  in our experiment;  $v_{ref}(n) = r(nT)$ . The sampled amplitudes are denoted as  $v_{ref}(n)$  and are indicated in Fig. 1(a). These amplitudes are converted into delay times

$$\tau^B(n) = \left[ \frac{v_{ref}(n) - v_{ref}^{min}}{v_{ref}^{max} - v_{ref}^{min}} \right] \cdot (T - 2T_c) \quad (5)$$

with the remaining time in each sample cycle denoted as  $\tau^A(n)$ . These delay periods are shown in Fig. 1 on the time scale between (b) and (c).

The charge accumulated during  $\tau^A(n)$  is transferred into the "negative" A shift register (shown in the device diagram, (Fig. 2) and similarly  $\tau^B(n)$  charges are transferred into the "positive" B register. When the CCD output is processed, the difference represents both positive and negative excursions of the accumulated product.

Because the charge is shifted past two photo-gates during each shift register clock cycle of  $\phi_1$  and  $\phi_2$ , double transfer pulses, shown in Fig. 1 (b) and (c), must be used to completely empty the photocharge into the shift registers during each time  $T_c$ .

Note that one set of clock pulses occurs at a fixed interval  $T$ . At times  $t = nT + T + \tau^B(n)$ , there is another sequence which is not periodic; therefore, the term "semisynchronous" is coined to describe the method of clocking.

Following each shift  $\phi_1$ ,  $\phi_2$  (Fig. 1(d) and (e)), an output level set occurs (Fig. 1(f)). In our experimental system, a signal XTB (Fig. (8)) loads this output level into a waveform recorder (Model 805, Biomation, Cupertino, California). The waveform recorder samples, digitizes (8 bits), and buffers 2048 consecutive bytes, or output level samplings, from the CCD. The B and A outputs are interleaved in the recorded data.

For many applications, the speed of a dedicated analog processor (perhaps other CCD filters) would be preferable to digital processing. However, for our demonstration, we interfaced the 2048 bytes into a digital computer for simulation and freedom of data manipulation. The interleaved B and A register output generated by two spots of light being swept along the CCD with FM chirp convolution is shown in the graphical output from the computer, Figure 3.

Once in the computer, it is straightforward to take the difference between the alternate CCD outputs, thereby providing the negative-going waveforms previously discussed. This leaves us with 1024 bytes of information representing the time sequence of the convolution of the input image and the reference voltage signal. The output has some undesirable low frequency fluctuations. These appear to be related to an inability to separate charges into B and A registers as a function of position along the device. The "high" level of the transfer voltages,  $\phi_{XA}$  and  $\phi_{XB}$ , had some effect on these fluctuations and was chosen to minimize this problem. It must be appreciated that the particular CCD used was fabricated for use as an image sensor and that a design eliminating alternate photogates [Ref. 4] would simplify the requirements on the clocking waveforms and improve performance for convolver operation.

The low frequency fluctuations were removed by converting the time sequence into the frequency domain using a 1024-point Fast Fourier Transform (FFT) [Ref. 7] and then multiplying the real and imaginary parts of the discrete frequency representation by the function

$$M(k) = \begin{cases} \sin\left(\frac{\pi \cdot k}{50}\right); & k = 1, 2, \dots, 50 \\ 1; & k = 50, \dots, 976 \\ \sin\left(\frac{\pi \cdot (1026-k)}{50}\right); & k = 976, \dots, 1024. \end{cases} \quad (10)$$

$M(k)$  is shown in Figure 4 and the subsequent signal  $q(x_o, t)$  is shown in Figure 5.

To obtain the double spots of the original image from the data shown in Fig. 5, we simulated a bank of filters  $h_\ell$  with varying amounts of compensating dispersion. In the discrete frequency domain representation,

$$H_\ell(k) = \begin{cases} \exp[j2\pi(k-1)^2 \ell \times 10^{-5}] & \text{for } k=1, 2, \dots, 512; \\ 0 & \text{for } k=513; \\ \exp[j2\pi(1025-k)^2 \ell \times 10^{-5}] & \text{for } k=514, \dots, 1024. \end{cases} \quad (11)$$

The inverse transform of the CCD output using these filter functions was calculated for a variety of values  $\ell$ ; i.e., the calculated term was

$$F^{-1}\{Q(k) \cdot M(k) \cdot H_\ell(k)\}, \quad (12)$$

where  $F^{-1}$  is the inverse Fourier transform operator, and where  $Q(k)$  is the discrete transformed version of the CCD output signal. The inverse transform with maximum peak output and contrast was for  $\ell = 135$ . Figure 6 shows the magnitude (absolute value) of the final output. The existence of this output confirms the basic concept of operation of the input convolution.

For the experiment, the two spots of light were visually adjusted to give a separation of roughly half the length of the 256 element array. In Figure 6, the two peaks are about 70 units apart. Each unit corresponds to two photogate elements (due to the transfer/shift/transfer combination) so the two spots were actually separated by about 140 photogate spacings.

Maximum resolution, or the minimum width of the output spot, is essentially the inverse of the bandwidth of the recorded chirp. A reference chirp with a bandwidth of 0 to 25 kHz was used in order to provide at least two samples per cycle where each sample is  $T = 20 \mu\text{s}$ . The speed of the rotating mirror used to deflect the double spot was such that the image was on the CCD for only part of the chirp. This limited the recorded bandwidth to about 56% of the full chirp bandwidth. If we neglect negative frequencies, which arise since the Fourier transform of a real function is symmetric, and if we allow for 20% bandwidth compression between  $R(k)$  and  $R(\Delta v \cdot k)$ , for  $v \approx 0.2 v_i$ , then we expect the bandwidth to be about 230 units in the transformed domain. For each spot individually, a bandwidth of about 160 units was observed. This corresponds to the 6 or 7 units of width in the compressed pulses of Figure 3. Poor focusing and perhaps nonuniform velocity effectively widened the input image and caused rolloff in the transform domain in our experiment. Although the experimental setup was sufficient to demonstrate the basic principle of operation, it was not optimized to give quantitative results on resolution.

In addition to permitting the recording of images moving at an unknown velocity, there are several other attractive features which arise from this type of scanning. For example, saturation occurs not because of the brightness of an individual spot, but rather because of the average brightness of the image. Thus, effects of blooming from isolated bright spots would be reduced. Also, localized sources of dark current, which are not moving with the velocity of the image, would be smeared out. Images, whether real or created by

dark currents, that have different  $\Delta v$ 's will have different optimum matched filter functions, and will not compress concurrently.

In order to obtain the compressed image using Equation (11) and (12), many filters  $H_0$  had to be simulated and the optimum image selected. The auto-correlation of the image is more easily and directly obtained. The transformed output of the CCD is  $Q(\omega) = I(\omega) \cdot R(\omega)$  as described in Equation 8. From this, we can easily compute

$$|Q(\omega)|^2 = Q(\omega) \cdot Q^*(\omega) = I(\omega) \cdot R(\omega) \cdot R^*(\omega) \cdot I^*(\omega) \quad (13)$$

but since  $R(\omega) \cdot R^*(\omega)$  is a constant (in the ideal case), it can be omitted. Thus, Equation (13) gives the transformed image autocorrelation  $I(\omega) \cdot I^*(\omega)$ . Because the linear chirp drops out of the autocorrelation, the relative velocity  $\Delta v$  does not enter into the final result. The cross-correlation between two images separately scanned at the same velocity also possesses this characteristic of dropout of velocity information when processed; i.e.,  $I_1(\omega) \cdot R(\omega) \cdot R^*(\omega) \cdot I_2^*(\omega) = I_1(\omega) \cdot I_2^*(\omega)$ .

The role of the image function as input and of pulse-position modulation voltage as reference could be reversed, in which case the optical image can be used as a tap weighting function for a transversal filter acting on the sampling voltage input signal. For this application, the images should be spatially fixed. An optical transparency could be used to mask the array to provide fixed tap weights, or LED's individually focussed onto the sensors could be used to electronically vary the taps.

#### IV. CONCLUSIONS

The concept of performing convolution by modifying clocking waveforms in a charge coupled device image sensor has been illustrated experimentally. The mathematical implications of encoding an image by convolving it with a linear FM chirp point out several interesting capabilities: (1) Images can be integrated over long times even though moving with respect to the accumulating charge packets. A set of filters can be used to retrieve the original image. (2) The autocorrelation of such images is simply derived in spite of the motion. (3) Images moving with different velocities can be simultaneously recorded and subsequently separated with different compression filters subject to limitations in contrast and number of resolvable spots. Electro-optically controlled transversal filters can also be configured for a variety of applications using "semisynchronous" clocking.

We appreciate the direction of S. C.-C. Tseng at the start of this work, the help from A. J. Stein, A. A. Guido, S. Krasney, and C. G. Powell with the graphics terminal system and the computer interface, the design aid from T. R. Perry on the clocking circuits, and the comments on the manuscript from L. Kuhn.

#### REFERENCES

1. Séquin, C. H., and Tompsett, M. F., CHARGE TRANSFER DEVICES, Academic Press, New York,

1975.

2. Erb, D. M., and Nummedal, K., "Buried Channel Charge Coupled Devices for Infrared Applications," CCD Application Conf. Proc., Naval Electronics Laboratory Center, San Diego, pp. 157-167, September, 1973.
3. Texas Instruments, Inc., "Moving Target Sensor," Contract Report N00039-73-C-0070, October, 1973.
4. Lagnado, I., and Whitehouse, H. J., "Signal Processing Image Sensor Using Charge Coupled Devices," Int. Conf. Tech. and Appl. of CCD's, University of Edinburgh, pp. 198-205, September, 1974.
5. Cook, C. E., and Bernfeld, M., RADAR SIGNALS, Academic Press, New York, pp. 5-17, 130-172 (1967).
6. Rabiner, L. R., Schafer, R. W., Rader, C. M., "The Chirp Z-Transform Algorithm," IEEE Trans. Audio and Electroacoustics, AU-17, pp. 86-92, June, 1969.
7. McAuliffe, G. K., "APL Fast Fourier Program," RC 2832, IBM Thomas J. Watson Research Center, Yorktown Heights, N. Y. (1970).

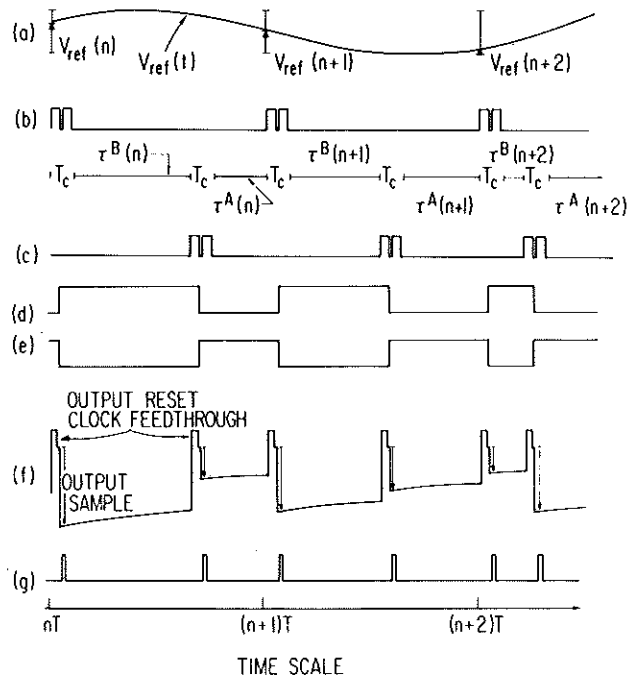


Figure 1. Semisynchronous waveforms for driving the CCD. (a) is the reference voltage waveform  $r(t)$  which is sampled at regular intervals. (b) and (c) are the transfer voltages,  $\phi_{XA}$  and  $\phi_{XB}$  respectively. (d) and (e) are the voltages  $\phi_1$  and  $\phi_2$ , respectively, which control the shift registers. (f) appears at the output stage of the CCD. The output information is sampled as indicated by the arrows occurring shortly after the reset. (g) is the external time base (XTB) control which advances the waveform recorder.

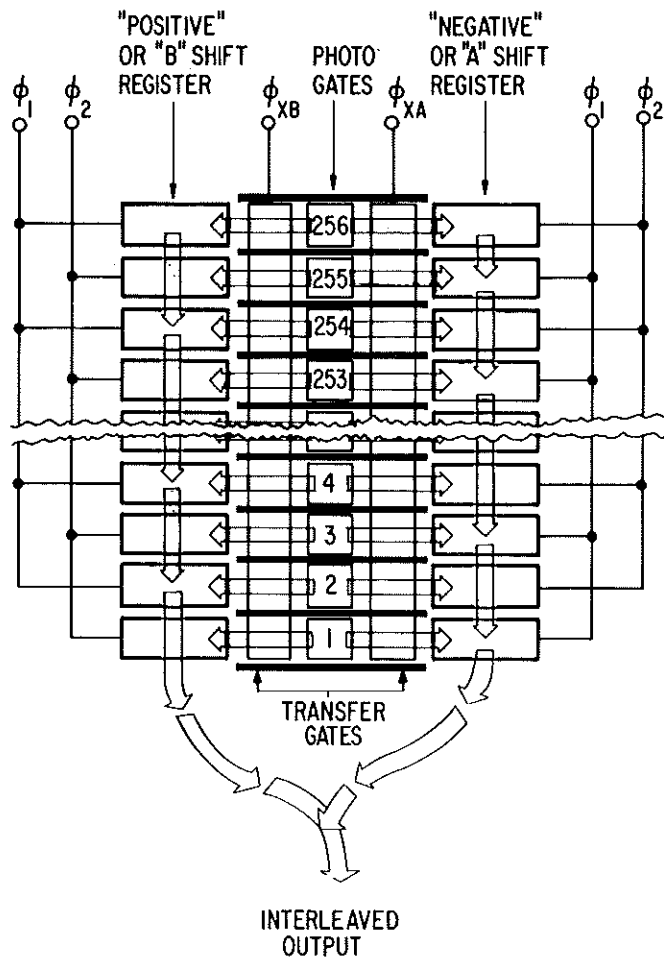


Figure 2. Schematic layout of the type of CCD used to sense and convolve images with reference voltage waveforms.

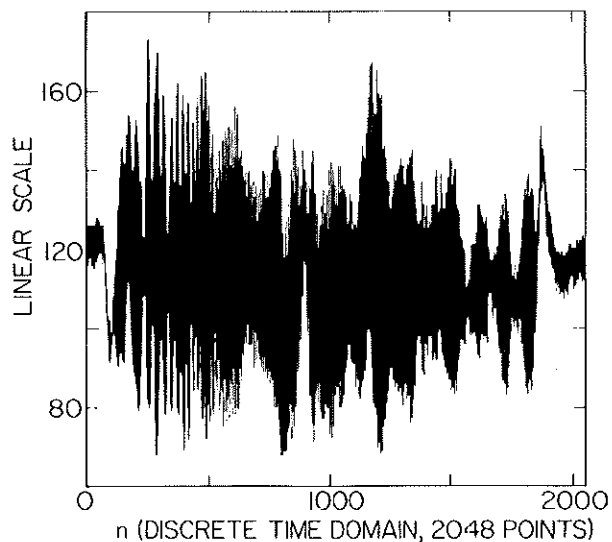


Figure 3. Output from the CCD after digital recording and as displayed on computer graphics system. Note that 2048 samples are shown. The "positive" and "negative" outputs are interleaved and will be later subtracted to provide 1024 samples of useful output.

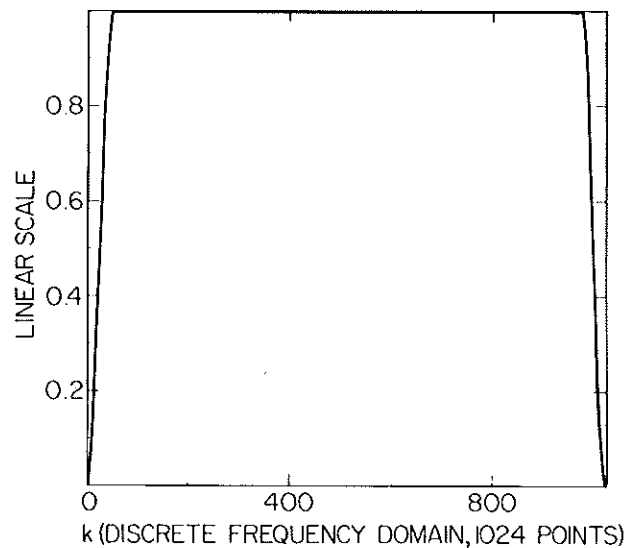


Figure 4. Transformed low frequency rejection filter  $M(k)$ . Due to cyclic behavior of the discrete Fourier transform, negative low frequencies appear at right end of the scale.

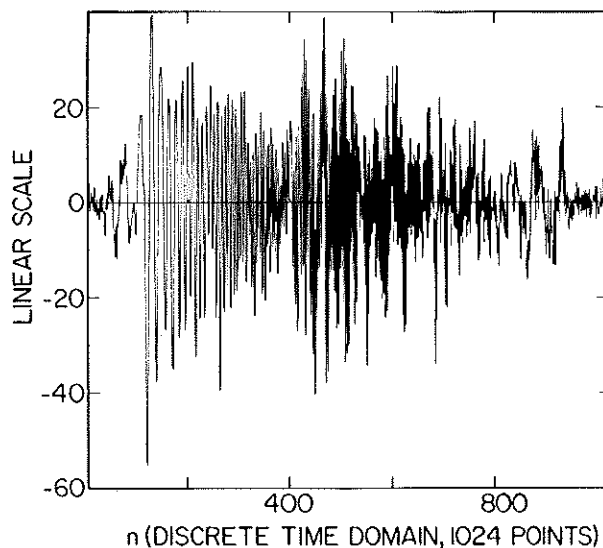


Figure 5. CCD output after "positive" and "negative" terms are combined and low frequency components have been removed.

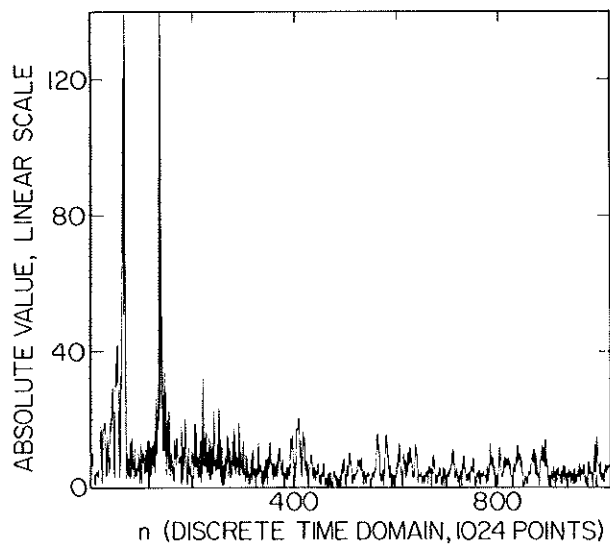


Figure 6. Magnitude of the output after final compression by simulated matched chirp filter. The two peaks correspond to the two spots originally scanned along the CCD sensor.